

A critical examination of the turbulence instrument used in the Marsta micro-meteorological field project

By ULF HÖGSTRÖM, *Department of Meteorology, University of Uppsala, Uppsala, Sweden*

(Manuscript received December 20, 1973; revised version April 24, 1974)

ABSTRACT

A turbulence instrument described earlier (Högström, 1967), and used in an extensive micro-meteorological field project, has been examined critically. Static wind tunnel calibrations give accurate, reproducible results. Field measurements and theoretical considerations indicate complications in the dynamical situation, however. It is shown that the instrument is well suited for the measurement of the horizontal component of the wind and its rapid fluctuations. For the measurement of the turbulent fluxes of sensible heat and of water vapour a correction of order of magnitude 10 % must be applied. The instrument is further shown to be unsuited for measuring the shearing stress and the variance of the vertical velocity component

1. Introduction

In the Marsta micro-meteorological field project a large number of experiments (see Högström, 1974) were performed with the turbulence instrumentation shown on Fig. 1. It consists of three parts: a wind instrument, one 'dry' thermometer and one 'wet' thermometer. The latter two instruments are exactly the same as the corresponding parts in the first presentation of this turbulence instrumentation (Högström, 1967), and their behaviour is well known (see Smedman-Högström, 1973). This report will concentrate entirely on the wind measuring equipment.

The version of this instrument used in the Marsta project is in principle not different from the original version, presented in Högström (1967). Thus, it consists of a wind vane with two pair of plates, one oriented vertically, the other horizontally, as shown in Fig. 1. Each pair of plates consists of three parts (see Fig. 2): (1) A rectangular block of plexiglass which is fixed to the instrument; (2) Two elastic beryllium copper strips (0.2 mm thick), fixed to the plexiglass block at one end; (3) Two rectangular plates ($36 \times 54 \times 0.5$ mm) of superpertinax which are fixed to the free ends of the beryllium copper strips. On both sides of these strips 600 Ω strain gages have been glued, which are connected in a Wheatstone bridge.

In Högström (1967) certain results of *static* wind tunnel calibrations were given. Calibrations of this kind has been repeated, and this time in a much bigger wind tunnel where the entire instrument could be inserted in the test section (the earlier calibrations were performed in a small tunnel where only a pair of plates could be inserted). The results of these calibrations are given in the next Section. However, analyses of the field experiments performed at Marsta, clearly indicated that these *static* calibrations did not tell the whole story about the instrument. Therefore a critical examination of the *dynamical* behaviour of the instrument was carried out. This study is presented in Section 3.

2. Static calibrations

The calibrations were performed in the low-speed wind tunnel of the Department of Aeronautics of the Royal Institute of Technology in Stockholm. The tunnel is of the closed-circuit type, with a 4.6 meter long test section and octagonal cross section, 2.1 m wide and 1.5 high. The turbulence level in the test section is very low, so the flow can be considered laminar for our purposes. The whole instrumentation (including the thermometers) was placed in the tunnel. The shaft was fixed to a pivot, so that the whole instrument could be tilted

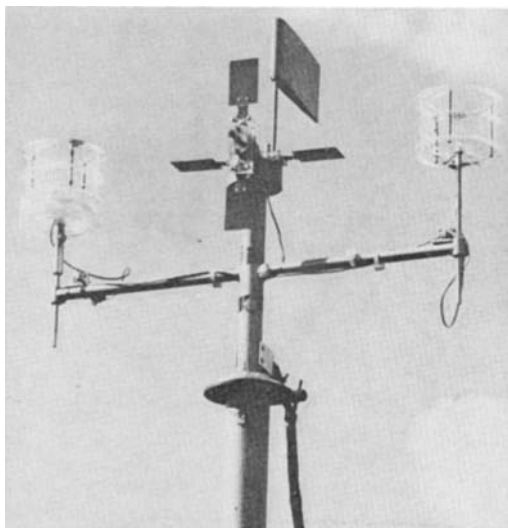


Fig. 1. The turbulence instrument used in the Marsta micro-meteorological field project. Resistance thermometers for 'dry' and 'wet' temperature to the right and left respectively.

about a horizontal axis perpendicular to the flow, in order to obtain a 'vertical' wind component, i.e. a wind component along the instrumental axis.

For the sake of simplicity, the following notions are introduced:

the x -plates = the vertically oriented pair of plates

the x -signal = the signal from the x -plates

the z -plates = the horizontally oriented pair of plates

the z -signal = the signal from the z -plates.

In strictly horizontal flow the z -signal is of course zero, and the wind speed is obtained from the x -signal. In Högström (1967) it was shown that the output from the plates at perpendicular attack is proportional to the square of the wind speed, i.e.

$$U_0 = \sqrt{\frac{x}{b_x}} \quad (1)$$

where b_x is an instrumental constant, the index x referring to the x -signal. Several calibrations in the interval 0.5–15 m/s indicate that this relation holds within the accuracy that the wind tunnel speed can be determined.

Tellus XXVI (1974), 6

The stability of the calibration could be checked regularly by a very simple method: A series of plates were made out of widely different materials (paper, plastic, aluminium and copper) and of different thickness but of exactly the same size (36×54 mm) as the wind sensing plates. These plates were made in pairs, so that two identical test plates could be placed on the two plates of the instrument, which were now placed horizontally in a special supporter. Now, a certain pair of test plates gave rise to a signal corresponding to a certain wind speed. The series of testplates was designed as to correspond to ten different wind speeds in the range 0.5–15 m/s. These checks showed a remarkable constancy in the calibration constants, b_x and b_z , of the different pairs of plates used during the project (b_z is the instrumental constant of the

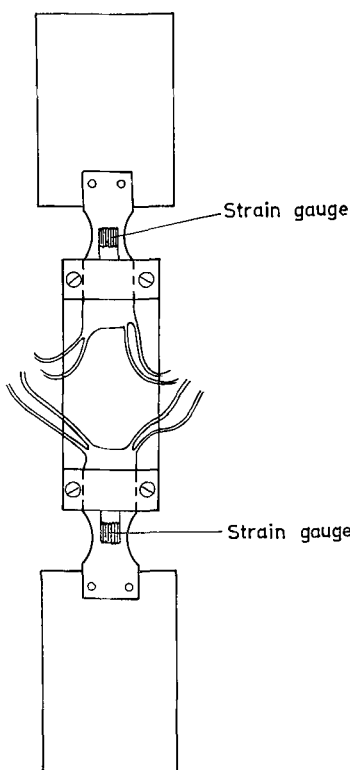


Fig. 2. A pair of wind-sensing plates. The outer rectangular plates are fixed to elastic beryllium copper plates, which in turn are fixed to the central plastic block. The bending of the elastic plates is transmitted to electrical signals by strain gauges glued on both sides of the plates. (From Högström, 1967.)

z -plates, corresponding to b_x , i.e. the quotient between the z -signal and the squared wind speed at perpendicular attack).

The behaviour of the instrument at other angles of attack than 90° was tested carefully at several occasions. The first and important result, reported already in Högström (1967), is that the quantity

$$f(\varphi) = x(\varphi)/x(90^\circ) \quad (2)$$

is independent of the wind speed and the same for all pairs of plates (of the same shape). This implies that if the wind has an inclination φ to the horizontal the modulus, U , of the wind vector is obtained by combining eqs. (1) and (2):

$$U = \sqrt{\frac{x}{b_x \cdot f(90^\circ - \varphi)}} \quad (3)$$

It also implies that

$$\frac{z}{x} \frac{b_x}{b_z} = \frac{f(\varphi)}{f(90^\circ - \varphi)} = G \quad (4)$$

is also a function of φ only. If the function $G = G(\varphi)$ is known, the angle φ can thus be obtained from the x -, and z -signals, according to eq. (4), and then the Cartesian components of the wind vector are respectively:

$$\left. \begin{aligned} u &= U \cos \varphi \cdot \cos \psi \\ v &= U \cos \varphi \cdot \sin \psi \\ w &= U \sin \varphi \end{aligned} \right\} \quad (5)$$

where ψ is the azimuth deviation from the mean wind direction during a run. This angle was obtained as the output from a low friction potentiometer coupled to the vane.

The function $G(\varphi)$ is very complicated. Fig. 3 shows the results of a detailed calibration in the range $-60^\circ \leq \varphi \leq 60^\circ$. The curve has been obtained as a result of both rising and falling series of φ -s, and the result is no doubt fully reproducible.

The curve of Fig. 3 can easily be adapted to a form convenient for use with a computer. A complication of more fundamental nature is the fact that there are three φ -values for each G -value in two ranges: $+21^\circ < \varphi < +33^\circ$ and $-35^\circ < \varphi < -17^\circ$. This is, however, of very little practical importance. It is possible to show, by

a straightforward analysis that if the computer is instructed to make a random choice between the three possible φ -values corresponding to a certain G -value, the error introduced in the determination of the turbulent fluxes is very small: If the standard deviation of φ is 10° , the error is ca. 0.02% and if the standard deviation is 20° or 30° the error is about 0.1%. The details of that analysis are omitted here, as other errors, described in the next section, are of far greater magnitude.

3. Behaviour of the instrument in the dynamical situation

At a few meters' height over an extensive, flat site the mean vertical wind component is very close to zero for a measuring period of the order of half an hour. Then the corresponding mean value for the z -signal, \bar{z} , should also be very close to zero. The lack of symmetry of the $G(\varphi)$ -curve, as evident in Fig. 3 can be shown to introduce a very small zero offset. In the actual runs \bar{z} is in general far from zero. When these measured \bar{z} -values (normalized for possible differences in b_z) for the different runs are plotted against the mean wind speed, Fig. 4 is obtained. The crosses are for unstable and near neutral and the rings for stable stratification. Apparently the \bar{z} -values are closely correlated to the mean wind speed of the runs, particularly for the unstable cases. This zero offset for the z -signal is so large that it cannot be explained in terms of any reasonable 'static' effect one can think of. It is necessary to review the behaviour of a flat plate exposed to a *changing* flow. The following general discussion is based on Batchelor (1967).

If a flat plate is *suddenly* exposed to a flow that makes a certain angle to its plane, the streamline pattern is of the type shown in Fig. 5a: the pattern is entirely symmetrical, with one stagnation point near the leading edge on the lower side and another stagnation point near the trailing edge on the upper side. In this initial stage the circulation around the plate is zero and hence the lift force is also zero, because

$$\text{lift force} = (\text{density of the air}) \times (\text{velocity of the air}) \times (\text{circulation})$$

Now this situation cannot exist in equilibrium.

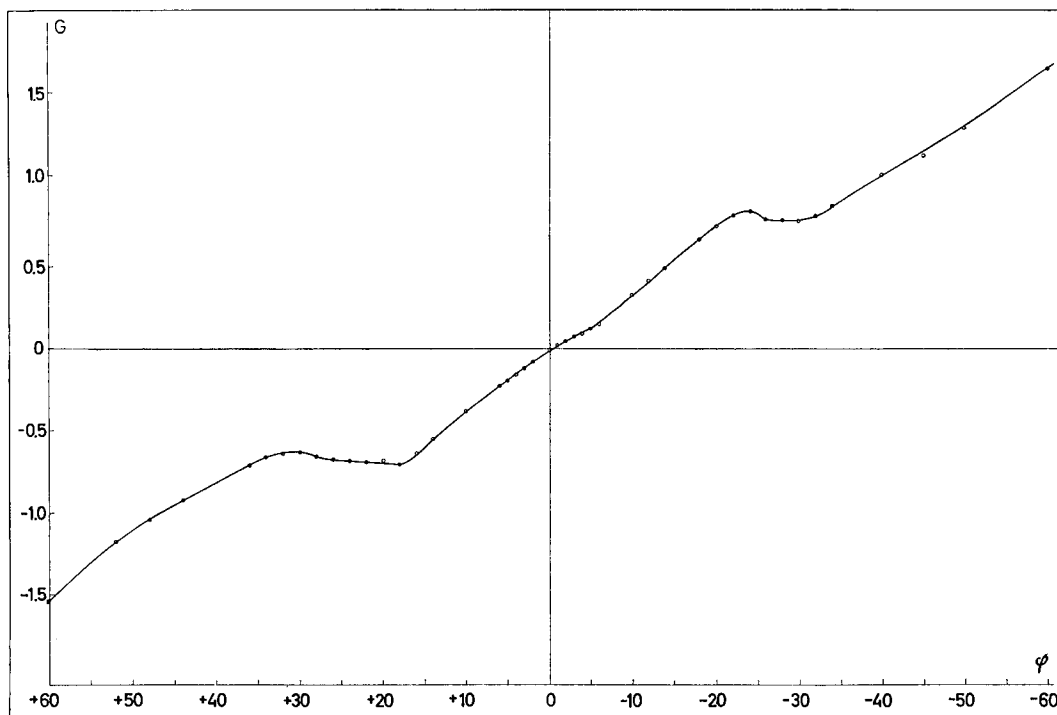


Fig. 3. Angular response of the turbulence instrument in static calibration. φ is the angle between the flow and the plane of the z -plates. The ordinate gives the function $G(\varphi)$.

A boundary layer separation takes place on the upper side of the plate, which results in the formation of a vortex at the trailing edge (Fig. 5*b*). Next, this vortex is swept away by the flow (Fig. 5*c*). As the circulation around an area enclosing the plate and the vortex (ABCD-EF) is zero, the circulation left around the plate (ABEF) is equal in magnitude but opposite in sign to the circulation around the vortex (BCDE). Now the flow pattern has changed to the new, non-rotational equilibrium state of Fig. 5*d*: the upper stagnation point has moved to the trailing edge, making the velocity there finite.

During the course of events described above, the circulation (and hence the lift force) changes from zero to an equilibrium value. But the z -signal is proportional to the lift force and should thus vary accordingly. This means that every time the wind vector changes rapidly, a systematic error in z arises. If the accelerations are not symmetrically distributed between up-winds and down-winds, this would result in a \bar{z} which is different from zero, as found (Fig. 4).

To analyse the influence of the above discussed effect on the turbulent fluxes, the following notions are introduced:

$$z_m = z_t + \Delta z$$

$$\varphi_m = \varphi_t + \Delta \varphi$$

$$w_m = w_t + \Delta w$$

where the index m refers to measured quantities and t refers to 'true' quantities. From eq. (4):

$$G(\varphi_m) = \frac{z_t}{x} \frac{b_x}{b_z} + \frac{\Delta z}{x} \frac{b_x}{b_z}$$

and we introduce the new notion

$$\Delta G = \frac{\Delta z}{x} \frac{b_x}{b_z}$$

Then we can write

$$\Delta \varphi = \frac{d\varphi}{dG} \Delta G = \frac{1}{G'} \frac{\Delta z}{x} \frac{b_x}{b_z} \quad (6)$$

with $G' = dG/d\varphi$.

The last of eqs. (5) gives:

$$\begin{aligned}
 w_m &= U \sin(\varphi + \Delta\varphi) = U \sin\varphi \cos\Delta\varphi \\
 &+ U \cos\varphi \sin\Delta\varphi \approx w_t(1 + \Delta\varphi) + U(1 + \varphi)\Delta\varphi \\
 &= w_t + 2 \frac{w_t \Delta z}{G' U^2 b_z} + \frac{\Delta z}{G' U b_z} \quad (7)
 \end{aligned}$$

where eqs. (1) and (6) have been used.

First we will use the result, eq. (7), to seek an expression for the error in the variance of the vertical velocity, w^2 :

$$\begin{aligned}
 \overline{\Delta w^2} &= \frac{\overline{\Delta z^2}}{G'^2 b_z^2} \left(\frac{1}{U} \right)^2 \left(4 \frac{w_t^2}{U^2} + 1 + \frac{4w_t}{U} \right) \\
 &+ \text{correlation terms}
 \end{aligned}$$

If we skip the correlation terms and put $\overline{\Delta z^2} = (\overline{\Delta z})^2$, we can make a rough estimation of $\overline{\Delta w^2}$ at different wind speeds, taking $\overline{\Delta z}$ from Fig. 4, and inserting typical values from the runs. The result is that the error is very large for low wind speeds: for $\bar{U} = 2$ m/s $\overline{\Delta w^2} = 0.64$ m²/s². It then decreases rapidly with increasing wind speed, being only ca. 0.006 m²/s² at $\bar{U} = 5$ m/s.

Multiplying eq. (7) throughout by u' and rearranging terms, makes an expression for the error in $\overline{u'w'}$:

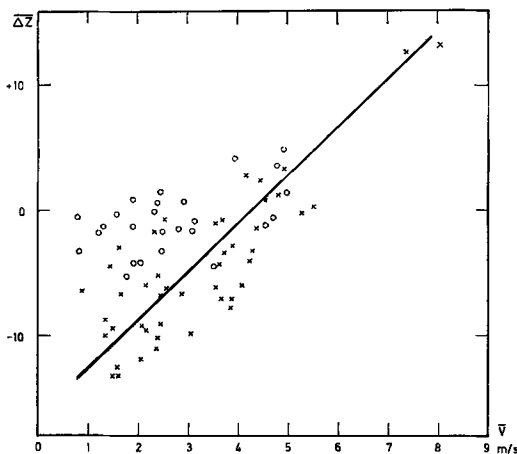


Fig. 4. Run-mean offset of the z -signal as a function of run-mean wind speed. The line has been fitted by eye to the crosses which represent unstable or near-neutral runs. Rings represent stable stratification.

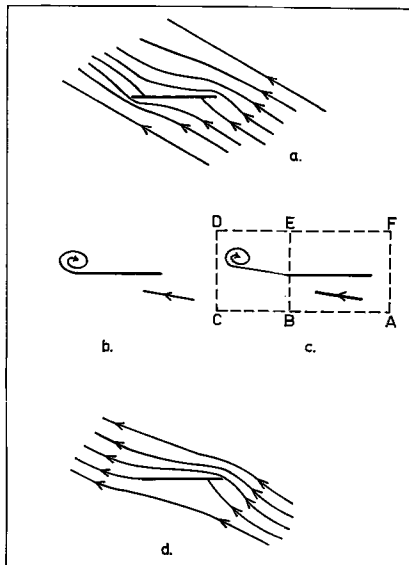


Fig. 5 a-d. A thin plate in a starting flow. (After Batchelor, 1967.)

$$\begin{aligned}
 \Delta(\overline{u'w'}) &= \overline{u'w_m} - \overline{u'w_t} = 2 \left(\frac{\overline{u'w_t \Delta z}}{(\bar{u} + u')^2} \right) \frac{1}{\bar{G}' b_z} \\
 &+ \left(\frac{\overline{u' \Delta z}}{\bar{u} + u'} \right) \frac{1}{\bar{G}' b_z}
 \end{aligned}$$

With the following approximation

$$\begin{aligned}
 \left(\frac{1}{\bar{u} + u'} \right) &\approx \frac{1}{2} \left(\frac{1}{\bar{u}^2 + u'^2 + 2\bar{u}u'} + \frac{1}{\bar{u}^2 + u'^2 - 2\bar{u}u'} \right) \\
 &= \frac{1}{\bar{u}^2 - u'^2} \quad (8)
 \end{aligned}$$

the above expression becomes:

$$\begin{aligned}
 \Delta(\overline{u'w'}) &= \frac{\overline{2u'w' \Delta z} + \overline{\bar{u}u' \Delta z} - \overline{u'^2 \Delta z}}{\overline{u'^2 \Delta z}} \\
 &\quad \underbrace{\hspace{10em}}_A \\
 &\quad \times \underbrace{\frac{\overline{u'^2 \Delta z}}{G' b_z (\bar{u}^2 - u'^2)}}_B \quad (9)
 \end{aligned}$$

The error in $\overline{u'w'}$ is thus expressed as a product between two factors: A which contains correlation

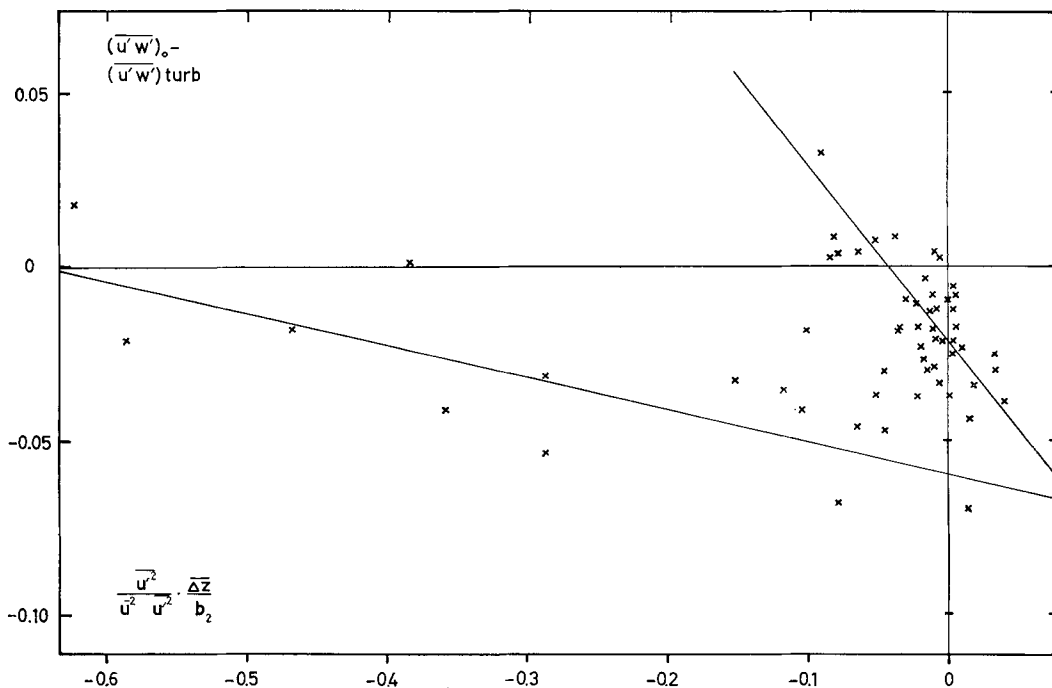


Fig. 6. The error in the turbulent measurement of $\overline{u'w'}$ as a function of the quantity B of eq. (9). $(\overline{u'w'})_o = -u_*^2$, which has been determined from low-level mean wind measurements by a stability dependent 'skin friction method' (Högström, 1974).

tions between the fluctuating wind components and the fluctuating error in the z -signal, and B , which only contains quantities which are explicitly evaluated during each run. B can thus be determined for each run in contrast to A .

In Högström (1974) is described how $u_*^2 = -\overline{u'w'}$ is determined from measurements of mean wind speed (measured by a cup anemometer) at a low level (1.14 m). As there are reasons to believe that these measurements are fairly accurate, we could use them as a reference for comparison with the corresponding data obtained with the direct method, that is to say that

$$(\overline{u'w'})_m - (\overline{u'w'})_o = \Delta(\overline{u'w'}) \quad (10)$$

where $(\overline{u'w'})_o$ is the value obtained from the cup anemometer evaluations and $(\overline{u'w'})_m$ is obtained from the turbulence instrument in the same run. The quantity (10) has been plotted in Fig. 6 against the quantity B of eq. (9) for all the Marsta runs. The following conclusions seem justifiable: The error in $|\overline{u'w'}|$ can be very

large—often bigger than $|\overline{u'w'}|$ itself. The data points in Fig. 6 appear to order themselves along the two different lines drawn in the Figure. It is reasonable to suppose that one could find some criteria (such as stability) which would make it possible to decide conclusively to which of the two groups of points a certain run belongs. This has not been tried, however. The reason for this is that Fig. 6 does not form a very convenient basis for correcting measured $\overline{u'w'}$ -values, even if it could be determined for sure which line should be used in a given case—the correction is in general of the same order of magnitude as the quantity to be corrected and the scatter is large. It is much better then to use the values determined by the cup anemometer measurements, used as a reference in this comparison.

Multiplying eq. (7) throughout by the temperature fluctuation, T' , and rearranging terms, makes an expression for the error in $\overline{w'T'}$:

$$\Delta(\overline{w'T'}) = (\overline{w'T'})_m - (\overline{w'T'})_t = \left(\frac{\overline{w'T'\Delta z}}{(\bar{u} + u')^2} \right) \frac{1}{b_z G'}$$

$$\begin{aligned}
& + \left(\frac{\overline{w'T'\Delta z}}{(\bar{u} + \bar{u}')^2} \right) \frac{1}{b_z G'} \approx \frac{\overline{u'T'\Delta z} + 2\overline{w'T'\Delta z}}{(\bar{u}^2 - \bar{u}'^2) b_z G'} \\
& = \underbrace{\frac{\Delta z}{b_z G'(\bar{u}^2 - \bar{u}'^2)}}_C \underbrace{\frac{\overline{u'T'\Delta z} + 2\overline{w'T'\Delta z}}{\Delta z}}_D \quad (11)
\end{aligned}$$

This expression can be considered as a product of the two factors C and D , C containing only parameters which are evaluated for each run, while D is a triple correlation of which nothing can be said *a priori*.

In the Marsta project there was no independent determination of the flux of sensible heat, so we cannot plot the 'measured error' as we did for the shearing stress. But as net radiation, R , and ground heat flux, G , were measured, the sum of the fluxes of sensible heat, H , and of latent heat, EL_v , is known from the energy balance equation:

$$H + EL_v = R - G \quad (12)$$

It is possible to form an expression for the error in the measured water vapour flux which is exactly analogous to eq. (11) though with e , the water vapour pressure, substituted for the temperature, T . If we multiply that expression by L_v , add eq. (12) and divide by $[\overline{w'T'} + (\overline{w'e'}) L_v]$, we obtain:

$$\begin{aligned}
& \frac{\Delta[\overline{w'T'} + (\overline{w'e'}) L_v]}{\overline{w'T'} + (\overline{w'e'}) L_v} \\
& = \underbrace{\frac{\Delta z}{b_z G'(\bar{u}^2 - \bar{u}'^2)}}_C \frac{\overline{u'T'\Delta z} + (\overline{u'e'\Delta z}) L_v}{\Delta z[\overline{w'T'} + (\overline{w'e'}) L_v]} \quad (13)
\end{aligned}$$

Now

$$\frac{\Delta[\overline{w'T'} + (\overline{w'e'}) L_v]}{\overline{w'T'} + (\overline{w'e'}) L_v} = \frac{(H_m + Em L_v) - (R - G)}{R - G} \quad (14)$$

according to eq. 12. H_m and Em are the fluxes of sensible heat and of water vapour, measured with the turbulence instrument. They are not the raw fluxes, but the fluxes corrected for trend and for 'reduction in flux measuring efficiency'—see Högström (1974). The quantities R and G were not measured in all the Marsta

turbulence runs. In order to reduce the scatter in the diagram, only those runs were used for which $|R - G| \geq 30$ watts/m². In Fig. 7 the quantity (14) has been plotted against the quantity C of eq. (13). From the Figure can be seen that the relative error varies systematically with C , being in the mean about -10% for large negative C , zero for C somewhere around -0.5 and ca. $+30\%$ for the largest positive C -values encountered. A curve has been fitted by eye to the points in the diagram.

As the relative error of the mean is only of the order of magnitude 10% and the scatter of the data points relative to the curve drawn is moderate, it is justifiable to use this curve for correction of the sum $(H + EL_v)$. It is known that the correlation between the temperature-, and the humidity fluctuations is very high over land surfaces (Swinbank & Dyer, 1967, measured a correlation coefficient $r_{Te} = 0.9$). It is reasonable then to assume that the curve in Fig. 7 is equally applicable to H and E separately as it is for the sum.

At a first glance it might seem surprising that the relative error in $\overline{w'T'}$ and $\overline{e'w'}$ is so small, considering the large relative error found in $\overline{w^2}$ (p. 674), at least for low wind speeds. But looking at eq. (13) and considering the previous discussion in this paper, it is perhaps not so strange: It has been well documented that the instrument measures the vertical wind component very accurately during stationary conditions—it is accelerations that cause the erroneous z of eq. (13), and there seems to be no physical reason to expect a close correlation between accelerations of the horizontal wind and the instantaneous quantities $u'T'$ and $u'e'$. This triple correlation is apparently not zero, generally speaking, but it is clearly much lower than the corresponding correlations between $u'w'$ and z , between u' and z and between u'^2 and z , appearing in eq. (9), which cause the large error in $\overline{u'w'}$, illustrated in Fig. 6. It appears to be quite in order then to consider Fig. 7a relevant *in situ* calibration of the instrument for the measurement of $w'T'$ and $w'e'$, valid at least for use at the Marsta site.

As an application, consider the following case. The correlation coefficient between w and T can be expressed in the following manner:

$$r_{wT} = \frac{\overline{w'T'}}{\sigma_T \sigma_w} = \frac{\overline{w'T'}}{\sigma_T u_*} \frac{u_*}{\sigma_w} \quad (15)$$

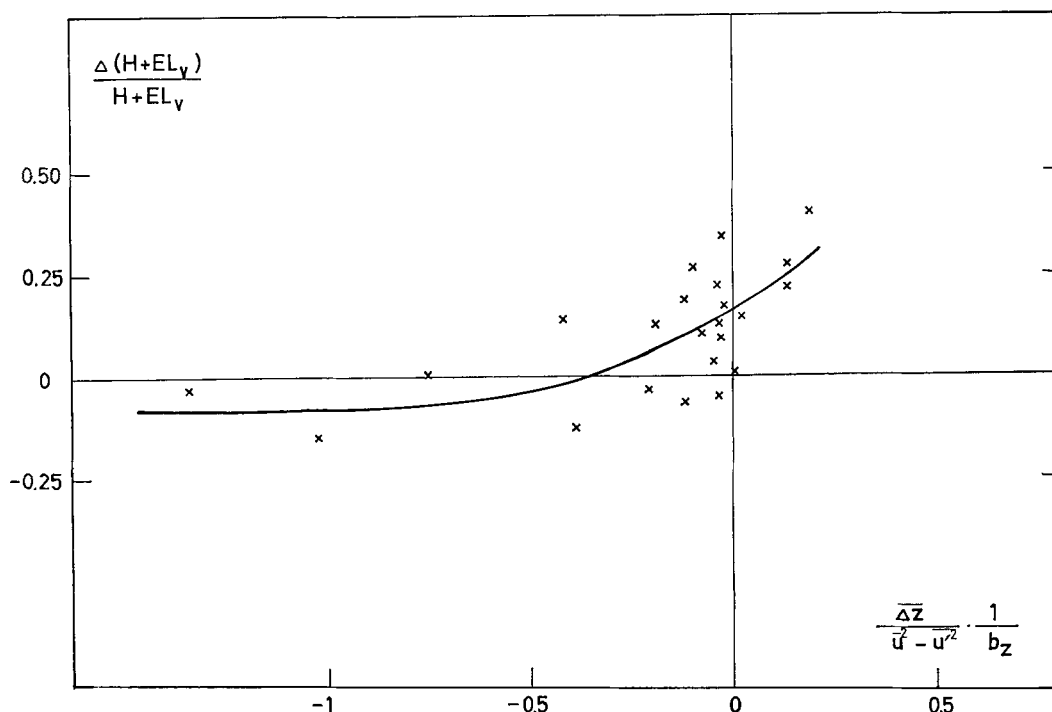


Fig. 7. The relative error in the turbulent measurement of $(H + EL_v)$ as a function of the quantity C of eq. (13).

This quantity is expected to show Monin-Obukhov similarity in the surface layer, i.e. it should be a function only of z/L , where z is height above ground and L is Monin-Obukhov's length $= -T u_*^3 / (k g \overline{w'T'})$. Of the quantities constituting eq. (15) $\overline{w'T'}$, σ_T and u_* have been determined directly from the measurements at Marsta and so has L . The quantity u_*/σ_w , however, was determined from Fig. 1 of Wyngaard et al. (1971). The result is shown in Fig. 8, the rings being data measured at 3 m and the crosses data from 12 m. This result agrees very well with that obtained by Haugen et al. (1971), their Fig. 11 (if the Richardson number, Ri , of their plot is converted to z/L with the aid of the relation obtained by the Kansas group in Businger et al. (1971). The r_{wT} -plot of Fig. 8 contains data from many runs which are not included in constructing the 'calibration curve' (Fig. 7).

The accuracy obtained for the fluxes measured with the instrument discussed here should be regarded in relation to the results obtained during the Tsimlyansk comparison (Tsvang et

al., 1973), where different types of turbulence instruments were run in parallel. The comparison revealed systematic errors in some of the instruments due to difficulties to maintain electronic stability of the complicated measuring systems, which were of about the same magnitude as the systematic errors found in this study. After correcting for the systematic errors remaining, occasional differences in $\overline{w'T'}$ obtained with the instruments were of order 10% in the Tsimlyansk study. As described earlier in this paper, the Marsta turbulence instrument is electronically extremely simple and retains its static calibration very well (p. 671). In view of what has been said above it is to be expected that the occasional error in the determination of $\overline{w'T'}$ or $\overline{w'e'}$ is not greater than ca. 10%.

The 'lift force error' discussed in Section 3 is only active for angles of attack less than a certain, comparatively small value. At larger angles of attack there is another flow regime. This should almost always be the case for the x -plates, and as the horizontal component of the wind is determined almost entirely by the x -

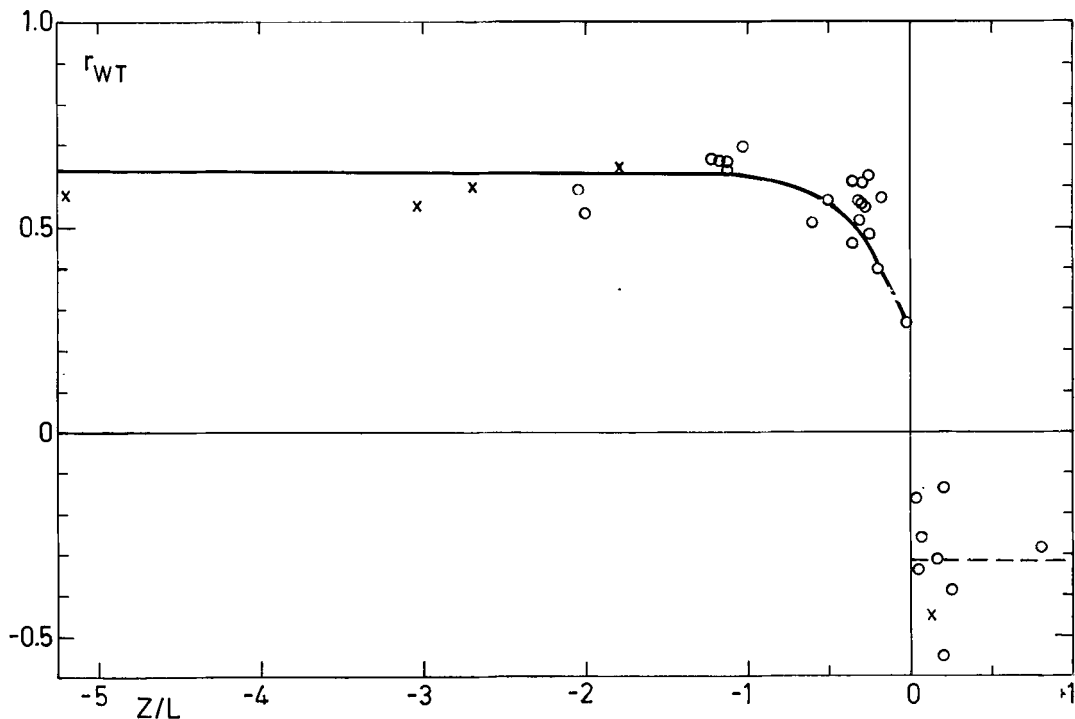


Fig. 8. Correlation coefficient r_{wT} as a function of z/L . \circ , runs from 3 m; \times , runs from 12 m.

signal (see eqs. 3 and 5), we conclude that the u - and v -statistics ($\overline{u'^2}$, $\overline{v'^2}$ and spectra of these quantities) are measured adequately by the instrument. The correctness of this assumption is verified by the analyses of the measurements. Fig. 9 shows two examples of u -spectra, one for

stable stratification ($z/L = 0.45$) and one for unstable stratification ($z/L = -0.23$). The spectra exhibit the features found by other investigators (see, e.g., Kaimal et al., 1972), in particular the two-thirds slope, predicted by the Kolmogorov theory for the inertial subrange.

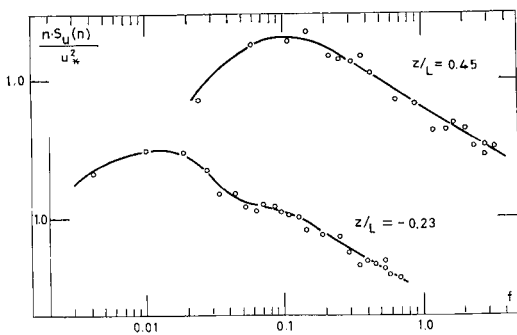


Fig. 9. Examples of u -spectra, measured with the Marsta turbulence instrument. On the abscissa $f = nz/\bar{V}$, where n is frequency, z height above ground and \bar{V} mean wind speed. On the ordinate $n S_u(n)/u_*^2$, where $S_u(n)$ is the spectral estimate and u_* = friction velocity. z/L = Monin-Obukhov dimensionless height.

4. Conclusions

The result of the critical examination of the Marsta turbulence instrument can be summarized in this way:

The instrument is *well suited* for measuring the horizontal component of the wind and its rapid fluctuations. By applying a correction of the order of magnitude 10% the following quantities *can easily* be measured: the turbulent flux of sensible heat, $H = \rho C_p \overline{w'T'}$, and the flux of water vapour, $E = \rho \overline{w'q'}$.

The instrument discussed in this paper is *not suited* for measuring the following quantities: the variance of the vertical velocity, $\overline{w'^2}$, and the shearing stress, $\tau = \rho \overline{u'w'}$.

Acknowledgements

This work has been sponsored by the Swedish Foundation for Scientific Research and Indu-

strial Development. The analyses of the u -spectra were performed by Dr Ann-Sofi Smedman-Högström.

REFERENCES

- Batchelor, G. K. 1967. *An introduction to fluid dynamics*. Cambridge University Press, London. 615 pp.
- Businger, J. A., Wyngaard, J. C., Izumi, Y. & Bradley, E. F. 1971. Flux-profile relationships in the atmospheric surface layer. *Journal of Atmospheric Sciences* 28, 181–189.
- Haugen, D. A., Kaimal, J. C. & Bradley, E. F. 1971. An experimental study of Reynolds stress and heat flux in the atmospheric surface layer. *Quarterly Journal of the Royal Met. Soc.* 97, 168–180.
- Högström, U. 1967. A new sensitive eddy flux instrumentation. *Tellus* 19, 230–239.
- Högström, U. 1974. A field study of the turbulent fluxes of heat, water vapour and momentum at a 'typical' agricultural site. To appear in *Quarterly Journal of the Royal Met. Soc.*
- Kaimal, J. C., Wyngaard, J. C., Izumi, Y. & Coté, O. R. 1972. Spectral characteristics of surface layer turbulence. *Quarterly Journal of the Royal Met. Soc.* 98, 563–589.
- Smedman-Högström, A. 1973. Temperature and humidity spectra in the atmospheric surface layer. *Boundary-Layer Meteor.* 3, 329–347.
- Swinbank, W. C. & Dyer, A. J. 1967. An experimental study in micro-meteorology. *Quarterly Journal of the Royal Met. Soc.* 93, 494–500.
- Tsvang, L. R., Koprov, B. M., Zubkovskii, S. L., Dyer, A. J., Hicks, B., Miyake, M., Stewart, R. W. & McDonald, J. W. 1973. A comparison of turbulence measurements by different instruments; Tsimlyansk field experiment 1970. *Boundary-Layer Meteor.* 3, 499–521.

КРИТИЧЕСКАЯ ПРОВЕРКА ПРИБОРОВ ДЛЯ ИЗМЕРЕНИЯ ТУРБУЛЕНТНОСТИ, ИСПОЛЬЗУЕМЫХ В МИКРОМЕТЕОРОЛОГИЧЕСКОМ ПРОЕКТЕ МАРСТА

Прибор для измерения турбулентности, описанный ранее Хогстромом (1967) и используемый в обширном микрометеорологическом проекте, подвергнут критической проверке. Статическая калибровка в аэродинамической трубе дала точный, хорошо воспроизводимый результат. Полевые измерения и теоретические соображения указывают, однако, на сложности, которые могут возникнуть в ди-

намической ситуации. Показано, что прибор хорошо приспособлен для измерения горизонтальных компонент ветра и их быстрых флуктуаций. Для измерений турбулентных потоков тепла и водяного пара следует применять коррекцию порядка 10 %. Далее показано, что прибор не годится для измерений напряжений трения и изменчивости вертикальной компоненты скорости.